We are IntechOpen, the world's leading publisher of Open Access books Built by scientists, for scientists

6,900
Open access books available

185,000
International authors and editors

200M
Downloads

154
Countries delivered to

Our authors are among the

TOP 1%
most cited scientists

12.2%
Contributors from top 500 universities

BOOK CITATION INDEX
CLARIVATE ANALYTICS
INDEXED

WEB OF SCIENCE™

Selection of our books indexed in the Book Citation Index
in Web of Science™ Core Collection (BKCI)

Interested in publishing with us?
Contact book.department@intechopen.com

Numbers displayed above are based on latest data collected.
For more information visit www.intechopen.com

Turbulence, Vibrations, Noise and Fluid Instabilities. Practical Approach.

Dr. Carlos Gavilán Moreno
Cofrentes N.P.P. Iberdrola S.A.
Spain

1. Introduction

Colloquially speaking, turbulence in any language means disorderly, incomprehensible, and of course, unpredictable movement. Consequently, we encounter expressions that employ the word turbulence in social and economic contexts; in aviation whenever there are abnormalities in the air, and even in psychology and the behavioural sciences in reference to turbulent conduct, or a turbulent life, in the sense of a dissolute existence. Thus has the word turbulence become associated with chaos, unpredictability, high energy, uncontrollable movement: dissipation. All of the foregoing concepts have their source in the world of hydrodynamics, or fluid mechanics.

In fluid mechanics, turbulence refers to disturbance in a flow, which under other circumstances would be ordered, and as such would be laminar. These disturbances exert an effect on the flow itself, as well as on the elements it contains, or which are submerged in it. The process that is taking place in the flow in question is also affected. As a result, they possess beneficial properties in some fields, and harmful ones in others. For example, turbulence improves processes in which mixing, heat exchange, etc., are involved. However, it demands greater energy from pumps and fans, reduces turbine efficiency and makes noise in valves and gives rise to vibrations and instabilities in pipes, and other elements.

The study of turbulence and its related effects is a mental process; one that begins with great frustration and goes on to destroy heretofore accepted theories and assumptions, finally ending up in irremediable chaos. "I am an old man now, and when I die and go to heaven, there are two matters on which I hope for enlightenment. One is the quantum electrodynamics, and the other is the turbulent motion of fluids. An about the former I am rather optimistic" (Attributed to Horace Lamb).

Nonetheless, some progress has been made in turbulence knowledge, modelling and prediction. (Kolmogorov, 1941). This chapter will deal briefly with these advances, as well as with the effects of turbulence on practical applications. In this sense, reference will be made to noise effects and modelling, as well as to flow vibration and instabilities provoked by turbulence. (Gavilán 2008, Gavilán 2009).

2. Turbulence.

Of itself, turbulence is a concept that points to unpredictability and chaos. For our purposes, we will deal with this concept as it applies to fluid mechanics. Therefore, we will be dealing

with turbulent flow. Throughout what follows, the terms *turbulence* and *turbulent flow* will be understood as synonymous. Some texts treat the terms *turbulence* and *vortex* as analogous, however, this seems to be rather simplistic. For the purposes of this work, it seems best to take the concept of turbulence in its broadest sense possible.

Historically, fluid mechanics has been treated in two different ways, namely, in accordance with the Euler approach, or pursuant to the Lagrange approach. The Eulerian method is static, given that upon fixing a point, fluid variations are determined on the effect they have on this point at any given time. On the other hand, the Lagrangian method is dynamic, given that it follows the fluid. In this way, variations in the properties of the fluid in question are observed and/or calculated by following a particle at every single moment over a period of time.

The Eulerian method is the one most employed, above all, in recent times, by means of numerical methods, such as that of finite elements, infinites, finite volumes, etc. Notwithstanding, there is great interest in the Lagrangian method or approach, given that it is one that is compatible with methods that do not use mesh or points. (Oñate, E; et al. 1996)

Throughout history, there have been two currents of thought as regards the treatment of turbulence. One is the so-called deterministic approach, which consists of solving the Navier-Stokes equation, with the relevant simplifications, (Euler, Bernoulli) practically exclusively via the use of numbers. The other approach is statistical. The work of Kolmogorov stands out in this field; work which will be dealt with below, given its later influence on numerical methods and the results of same. Apart from the Eulerian or Lagrangian methods, classic turbulent fluid theory will be dealt with in Section 2.1, whereas the statistical or stochastic approach will be dealt with in Section 2.2, in clear reference to Kolmogorov's theory. (Kolmogorov, 1941).

2.1 General theory

This section provides a brief and concise exposition of successive fluid flow approaches designed to respond to the presence of anomalies that were later referred to as *turbulence*, and which gave rise to the concept of turbulent fluid. Furthermore, the equations given enable the visualisation of the turbulence in question and its later development. A Eulerian and deterministic focus will be followed in this section.

Working in reverse to the historical approach, the fluid flow equation formulated by Navier-Stokes in 1820 is given; firstly, because it is the most general one, and secondly, because, of itself, its solution can represent the turbulent flow equation.

$$\frac{\partial u_i}{\partial t} + \sum_{j=1}^{n} u_j \frac{\partial u_i}{\partial x_j} = v\Delta u_i - \frac{\partial p}{\partial x_i} + f_i(x,t) \tag{1}$$

$$div\vec{u} = \sum_{i=1}^{n} \frac{\partial u_i}{\partial x_i} = 0 \tag{2}$$

$$u(x,0) = u^0(x) \tag{3}$$

Where u_i stands for the velocity components at each point and at each moment in time, v is the viscosity, p is the pressure at each point and at each moment in time, and f_i refers to the external forces at each point and at each moment in time. By annulling the viscosity and its effects, we get Euler's fluid flow equation announced in 1750.

$$\frac{\partial u_i}{\partial t} + \sum_{j=1}^{n} u_j \frac{\partial u_i}{\partial x_j} = -\frac{\partial p}{\partial x_i} + f_i(x, t) \tag{4}$$

$$div\vec{u} = \sum_{i=1}^{n} \frac{\partial u_i}{\partial x_i} = 0 \tag{5}$$

$$u(x, 0) = u^0(x) \tag{6}$$

In addition to this simplification, if we make the fluid stationary, so that:

$$\frac{\partial u}{\partial t} = 0 \tag{7}$$

we get the first Bernoulli theorem announced in 1738.

$$\frac{D}{Dt}\left(p + \rho \cdot \phi + \rho \frac{u^2}{2}\right) = 0 \tag{8}$$

The solving of these equations, given their simplifications and context conditions, provide us with a field of speeds and pressures for a fluid in movement. Indeed, as regards the Navier-Stokes equation, it can be solved and turbulences and instabilities determined by employing powerful numerical solution methods, such as that of the finite element.

Thus, the equations that govern fluid movement. By means of these two equations, particularly the last two (those of Euler and Bernoulli), it was observed that, under certain conditions, the results did not correspond to reality, on account of a certain problem of disorder developing in the fluid and its flow. Only the accurate and numerical solving of the Navier-Stokes equation can exactly reproduce these phenomena. To this end, resort must be had to potent computational fluid dynamic (CFD) software. Notwithstanding, in 1883, Osborne Reynolds discovered a parameter that predicted or anticipated the chaotic and turbulent of the fluid: the Reynolds number.

$$Re = \frac{\rho \cdot v_s \cdot D}{\mu} = \frac{v_s \cdot D}{v} \tag{9}$$

Thus was it established that the flow is stationary, and therefore laminar, for Re<2000 values, a fact which meant that the solutions given by Bernoulli and Euler were very accurate. For values of 2000<Re<4000 the system was deemed to be in transition, and therefore, not stationary. The functions that work best are those of Euler and Navier-Stokes. This turbulence undergoes three phases or states of development.

A. Growth of coherent bidimensional vortices[1].
B. Joining of Vortices
C. Separation of vortices and turbulent state in 3D

Finally, if completely turbulent, the fluid is non-stationary and tri-dimensinal for values of Re>4000. These solutions are only possible by means of using the Navier-Stokes equations.

In conclusion, only the numerical solution of the Navier-Stokes equation provides a solution that considers turbulence. Nevertheless, there are other processes and approaches that will be developed in Section 2.3. Turbulence is, therefore, produced by the interaction of the fluid with geometry, by the loss of energy due to viscosity, by density variations caused by temperature, or other factors, such as changes in speed, or all of these at once. Consequently,

---

[1] These are referred to as coherent because the vorticity is concentrated and the fluid flows around as if it were a solid obstacle. It keeps its shape for longer than a single rotation.

the turbulent flow is unpredictable and chaotic in the sense that it depends on a host of small variations in the initial conditions and these disturbances are amplified in such a way that it becomes possible to predict them in space and time. Another of its features is its great capacity for mixing and, lastly, that it affects at various scales and wavelengths. It could be said that together, fluid, structure and context conditions, constitute a non-linear, non-stationary dynamic system. Its most noteworthy characteristic is its sensitivity to the initial conditions and its self-similarity, which will serve as a staring point to develop Kolmogorov's theory.

In the 19th and 20th centuries, several researchers devoted great efforts to studying turbulence under certain, extremely particular conditions. Examples of such turbulence or instabilities are to those of Von Karman, Kevin-Helmotz, Raleygh-Bernard, and so on.

2.2 Kolmogorov´s theory

Kolmogorov's theory cannot be dealt with without first mentioning the spectral analysis of turbulence, or the application of Fourier's analysis to the study of turbulence. Fourier's theory decomposes the fluctuations into sinusoidal components and studies the distribution of the turbulent energy along several wavelengths. In this way it becomes possible to get several scales of turbulence and their evolution in time. This technique works and produces acceptable results when turbulence is homogenous. Under this condition, accurate equations can be determined for the speed spectrum and for the transferring of energy between difference scales of turbulence, as well as the dissipation of turbulent energy due to viscosity. The simplest development assumes that there is no average speed gradient, in such a way that the turbulence interacts with itself, with the energy dropping by itself. Neither energy sources nor sinks are taken into account.

To start, we assume that the speed of a particle in the fluid can be decomposed into an average speed plus a fluctuation component.

$$U_i = \overline{U_\iota} + u_i \tag{10}$$

R_{ij} is defined as the speed correlation function by the expression:

$$R_{ij}(x, x', t) = \overline{u(x, t)_\iota u(x', t)_J} \tag{11}$$

Given that we assume homogenous turbulence, R_{ij} is only a function of the distance r, which is the distance between x and x':

$$R_{ij}(r, t) = \overline{u(x, t)_\iota u(x', t)_J} \tag{12}$$

Therefore, we assume that the value of the correlation function tends to zero when the radius tends to the infinite. We now define a spectral function Φ_{ij} as the Fourier transform of the correlation function in 3D:

$$\emptyset_{ij}(k, t) = \frac{1}{(2\pi)^3} \int R_{ij}(r, t) \cdot e^{-ikr} \cdot d^3k \tag{13}$$

This spectral function, which will form the spectral matrix, depends on time and on the wave number k, which is a vector. The turbulent kinetic energy can be expressed as:

$$\frac{1}{2}\overline{u_\iota u_\iota} = \frac{1}{2}R_{ij}(0, t) = \frac{1}{2}\int \emptyset_{ii}(k, t)d^3k \tag{14}$$

The magnitude of the vector of the wave number $k=[k]$ is the inverse of the length, thus the length is k^{-1}. Therefore, if L is a characteristic scale of turbulence, the L^{-1} value of the wave number represents the higher scales of turbulence, where all the turbulent kinetic energy is contained. The spectral function, Φ_{ij}, describes the energy distribution in relation to wave numbers. It has a maximum value of $[k]=L^{-1}$, which drops to zero when $[k]$ tends to the infinite. The evolution of kinetic energy is defined as:

$$E = 2\pi k^2 \emptyset_{ii} \tag{15}$$

As far as the evolution of the k energy value is concerned, this can be seen in the following figure (Figure 1).
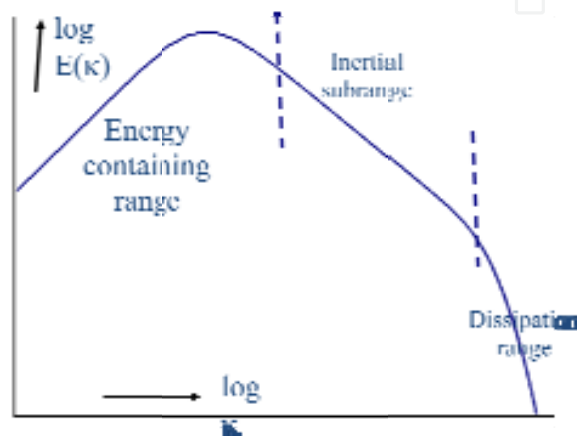

Fig. 1. Energy ranges.

This is where the term, or value, η comes in, referring to Kolmogorov's scale, which determines the scale point at which energy dissipation by viscosity is most significant. We will use the following equation for Kolmogorov's theory:

$$\frac{\partial E}{\partial t} = T - 2 \cdot \upsilon \cdot k^2 E \tag{16}$$

That is to say, the energy and its evolution in time will be a function of that which is transferred and that which is dissipated. Integrating it from k=0 to a greater, or finite, as well as limited, value gives us:

$$\frac{d}{dt}\int_0^k E(k'.t)dk' = -\aleph(k,t) - 2\upsilon\int_0^k k'^2 E(k',t)dk' \tag{17}$$

Where:

$$\aleph(k,t) = -\int_0^k T(k',t)dk' = \int_k^\infty T(k',t)dk' \tag{18}$$

This can be interpreted as follows:

"Energy changes in wave numbers below k on account of the interchange with larger wavelengths through the energy spectral fluid and the dissipation caused by viscosity forces on its own wavelength"

Kolmogorov holds that turbulence properties in the inertial range, above η, only depend on the energy spectral fluid, in such a way that:

$$\aleph = \bar{\varepsilon} \tag{19}$$

The idea behind this is that the transfer cascade evolves towards lower scales, leaving the spectral fluid as a fixed parameter. Consequently, the energy equation now stands at:

$$E(k,t) = C \cdot \varepsilon^{-\frac{2}{3}} \cdot k^{-\frac{5}{3}} \tag{20}$$

where C is a Kolmogorov constant, considered as a universal, the value of which is 1.5 when $L^{-1} << k << \eta^{-1}$ and the Re (Reynolds number) is high. Thus, beyond the inertial scale wave numbers, we have the dissipation range numbers, as shown in Figure 2.
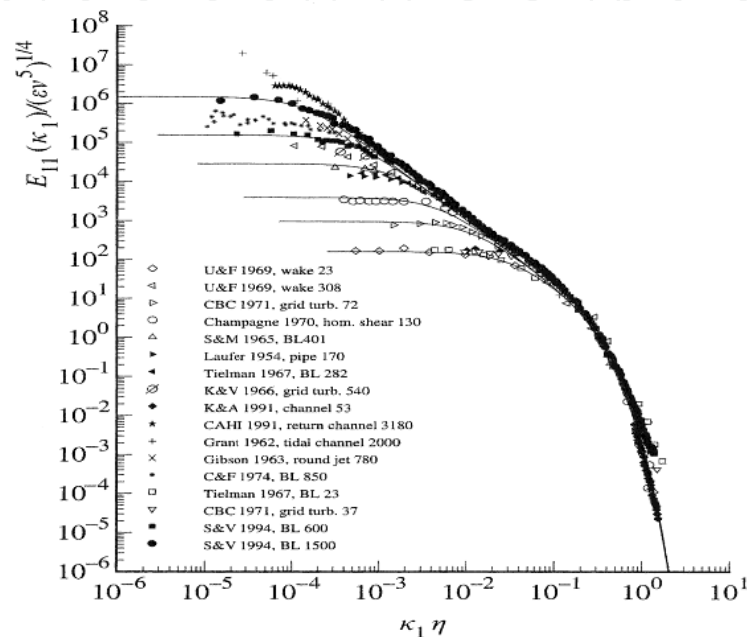

Fig. 2. Kolmogorov scales and data from several tests.

This range is only determined by the η parameter, which only has a dependence parameter, as shown by the equation (21).

$$\eta = \left(\frac{\upsilon}{\varepsilon}\right)^{\frac{1}{4}} \tag{21}$$

This Kolmogorov derived value gives the size of the smallest turbulence dissipation scale. The dissipation range energy expression now becomes:

$$E(k,t) = \varepsilon^{\frac{1}{4}} \upsilon^{\frac{5}{4}} \cdot F(k\eta) \tag{22}$$

where $F(\cdot)$ is also a universal function.

We will define the Kolmogorov time and speed scale factor with the ε y υ parameters, which determine the behaviour of the flow in the dissipation range:

$$t_\eta = \left(\frac{\upsilon}{\varepsilon}\right)^{\frac{1}{2}} \tag{23}$$

$$u_\eta = (\upsilon \cdot \varepsilon)^{\frac{1}{4}} \tag{24}$$

Thus, the Kolmogorov theory completes the spectral analysis. The theory postulates high Reynolds number values. The small turbulence scales are assumed that serve to balance and be controlled by the average energy flow, which is generated in the inertial scale and which equals the dissipation rate. Furthermore, Kolmogorov's theory universally predicts speed properties and their differences for small separations, as well as their correlations and spectre, only depending on the v y ε parameters. Kolmogorov also marked the boundary between the transferred or contained energy range (inertial range) and the dissipative structures by way of the following expression:

$$\frac{L}{\eta} = f(Re^{3/4}) \tag{25}$$

Therefore, given a Reynolds number, the lower scales are not sensitive to the turbulent flow in which they find themselves. Nevertheless, the lower scales are intimately related to the flow, with their properties varying substantially depending on the specific flow. These concepts will form the basis for future methods of modelling and solving fluid movement problems, such as *k-ε* and Large Eddy Simulation (LES) models.

2.3 Simulation of turbulent fluids.

As is well known, Navier, L.H.H. and Stokes, G.G derived fluid movement equations over 150 years ago. This equation, along with that of continuity, provides an answer to any fluid movement problem.

The solution and determination of the speed field is, therefore, nothing more than discretising the domain and the differential equations and applying context conditions in order to repeatedly solve the system formed until achieving convergence. This is the so-called Direct Numerical Solution (DNS). Nonetheless, this simple method is only useful in simple geometries, given that otherwise, the time calculation would be so big as to make any simulation unfeasible. This defect arises noticeably when we design fluid-structure (FIS) models. Consequently, other models need to be found, which are lest costly computationally speaking.

The most common solution to the high number of elements required by the former simulation method, DNS, is to use weighted, or weighting, techniques. In this way, modelling is done on a small scale expecting that the solution will respond to the flow as a whole. This is the idea that underlies the so-called Reynolds Averaged Navier-Stokes (RANS). It must be assumed that the speed of a turbulent flow can be described as follows:

$$\vec{u} = \bar{\vec{u}} + \vec{u'} \tag{26}$$

That is to say, as the sum of an average speed plus a fluctuating component on this average speed. The following is an example of the application of this assumption. It refers to the 2D modelling of a turbulent flow on a flat plate, the Navier Stokes (NS) equation for which is given below:

$$\rho \left(\frac{\partial u_x}{\partial t} + u_x \frac{\partial u_x}{\partial x} + u_x \frac{\partial u_x}{\partial y} \right) = \mu \frac{\partial^2 u_x}{\partial y^2} \tag{27}$$

replacing

$$\rho \left(\overline{u_x} \frac{\partial \overline{u_x}}{\partial x} + \overline{u_x} \frac{\partial \overline{u_x}}{\partial y} \right) = \mu \frac{\partial^2 \overline{u_x}}{\partial y^2} - \rho \frac{\partial}{\partial y} \overline{u'_x u'_y} \tag{28}$$

The difficulty of this expression and of all those assuming equation (28) is that an analytical expression of the term is required:

$$\rho \frac{\partial}{\partial y} \overline{u'_x u'_y} \tag{29}$$

known as Reynold Stress. In order to avoid this difficulty, the kinetic energy (k) and the dissipation rate (ε) are modelled. This gives rise to a well known model: the k-ε model. The simplification consists of the following:

$$\rho \cdot \overline{u'_x u'_y} = \mu_{turb} \frac{\partial \overline{u_x}}{\partial y} \tag{30}$$

where, moreover,

$$\mu_{turb} = \frac{C_k \cdot k^2}{\varepsilon} \tag{31}$$

by replacing all of this, in the proposed movement equation, the result is as follows:

$$\left(\overline{u_x} \frac{\partial \overline{u_x}}{\partial x} + \overline{u_y} \frac{\partial \overline{u_x}}{\partial y} \right) = v \frac{\partial^2 \overline{u_x}}{\partial y^2} - \frac{C_k \cdot k^2}{\varepsilon} \frac{\partial \overline{u_x}}{\partial y} \tag{32}$$

This k-ε model has a big advantage over the DNS model in that it takes less time to compute. This model provides acceptable solutions when flow fluctuations are not very important. When the flow motor, or the problem, to be studied has to do with pressure fluctuation, that is to say, external flow Flow Induced Vibrations (FIV), the RANS model is unviable, given that it does not provide quality solutions. There are several RANS model variations, the main features of which are shown in Table 1.

Method	Strengths	Weaknesses
Spalart-Allmaras	A one-equation model, which provides less computational effort than most other models. Produced for external flow over airfoils but is increasing in popularity for turbo machinery applications. Performs well for attached wall-bounded flows with weakly complex boundary layers.	Weak for adverse pressure gradients that produce boundary layer separation. Since it is relatively new, it has a lack of submodels available.
RNG k-ε	Possesses many of the same characteristics as the standard k-ε, but uses mathematical group theory to determine the previously empirical constants. It performs better for moderately complex flows like jet impingement.	Subject to limitations due to isotropic eddy viscosity assumptions.
Reynolds Stress Model (RSM)	Highly rooted in the physics by solving a transport equation for each Reynolds stress.	Requires much more computational effort than any other technique.

Table 1. RANS submodels, strengths and weaknesses.

Lastly, there is a model that lies halfway between the RANS and DNS. The DNS model has been seen to represent the real circumstance and disturbances very well. On the other hand, though the RANS model is extremely comfortable computationally speaking, it does not represent turbulence or disturbances very well. The so-called Large Eddy Simulation (LES) model provides instantaneous solutions, as does the DNS model, while at the same time containing models and simplifications such as those in the RANS model. The LES model solves the Navier-Stokes equation as does the DNS model, but the equations are spatially filtered, or refined. This filtering or refining of the equations means that the flow is determined at a characteristic scale, and is modelled afterwards at lower scales. It is the application of Kolmogorov's theory to non-stochastic numerical models.

This succession of modelling and refining is due to the fact that big eddies behave anisotropically and, therefore, must be calculated, whereas smaller eddies behave isotropically and can, as such, be treated statistically. Thus, the mesh is such that the majority of energy is contained in big eddies and calculated directly, the rest is assigned in a weighted manner to flow as a whole.

The bigger the Reynolds number, the bigger the cost in this LES model. Mathematically, the model is based on the Φ flow being formed by two superimposed flows:

$$\phi = \bar{\phi} + \phi' \tag{33}$$

the mesh flow, or the grand scale flow, $\bar{\phi}$
the sub-mesh flow, or the small scale flow ϕ'
The grand scale (GS) flow is calculated as follows:

$$\overline{\phi(x)} = \int \phi(x')G(x,x')dx' \tag{34}$$

where

$$G(x,x') = \begin{Bmatrix} \frac{1}{v} & \sqrt{x\epsilon\Delta v} \\ 0 \ resto \end{Bmatrix} \tag{35}$$

then replacing

$$\overline{\phi(x)} = \frac{1}{v}\int \phi(x')dx' \tag{36}$$

By applying these assumptions to the flow movement equation

$$\frac{\partial \overline{u_i}}{\partial t} + \frac{\partial}{\partial x}\left(\overline{u_i}\,\overline{u_j}\right) = -\frac{1}{\rho}\frac{\partial}{\partial x}\bar{p} + v\frac{\partial^2 \overline{u_i}}{\partial x_j^2} + \tau_{ij} \tag{37}$$

$$\tau_{ij} = \overline{u_i u_j} - \overline{u_i} \cdot \overline{u_j} \tag{38}$$

the latter term is modelled on the sub-mesh, or on the SGS sub-model and the accuracy of the model rests on the idea that lower speeds than the mesh are homogenous and, therefore, can be modelled with great accuracy. The aim of the LES method is to solve the majority of the flow and to model only a small part of it. Thus, the LES method strikes a balance between mesh size and accuracy. Figure 3, in which the solution for a turbulent flow in a pipe compares the RANS method with the LES one, provides an explanatory example.

These are practically the general models that are used in flow simulation and fluid movement. Notwithstanding, there are variations of these basic methods depending on the application in question.
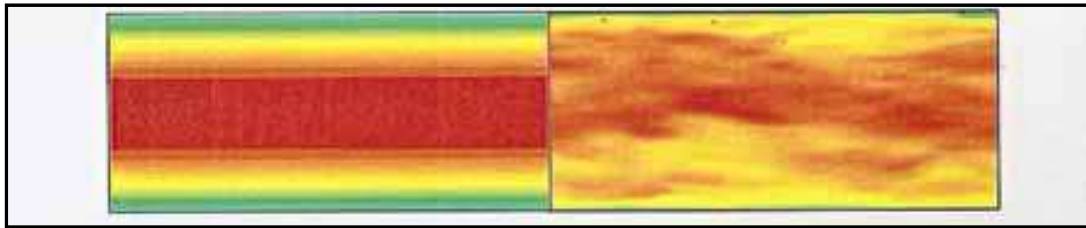
Fig. 3. Solutions of the same problem with a RANS model (on the left) and LES model (on the right).

Quite clearly, discretisations can be Eulerian, or Lagrangian, in such a way as to respond to both forms of tackling problems concerning fluid dynamics.

3. General effects of the turbulence. (FIC)

Having introduced turbulence, the turbulent flow and its equations and simulations, the question arises as to what can turbulence do? What are its possible effects? To answer these questions, first off it is necessary to decide whether the effects in question are general or local, that is to say, whether they are provoked by the turbulent flow or, on the contrary, are caused by turbulence or instabilities. The latter will be dealt with in Sections 4, 5 and 6, while the general effects are considered below.

Numerous studies have been carried out highlighting the benefits of turbulence with respect to miscibility, diffusion and heat exchange, though it can also have harmful effects. Here we are going to deal with the phenomenon of spontaneous cavitation, and its effects, in turbulent flow. Specifically, our aim is to study the effect of the change of speed caused by vorticity and pressure due to load loss on account of turbulence in high energy turbulent fluids near saturation point, such as, for example, feed water in power stations.

Firstly, we are going to define a non-dimensional parameter, which is called the cavitation number.

$$Ca = \frac{Pa - Pv}{\frac{1}{2}\rho v^2} \tag{39}$$

where:
P_a is the local or system pressure;
P_v is the vaporization pressure at system temperature;
P is the fluid density at system temperature;
V is the fluid speed.

Cavitation will occur when the parameter value is low. There is a limit value that corresponds to a determined speed, for each temperature and pressure, below which cavitation is ensured.

Speed can be defined in a turbulent flow as follows:

$$u_T(t) = u_m + \delta u(t) \tag{40}$$

That is to say, an average value and a fluctuation or oscillation component. Moreover, turbulence intensity is defined as:

$$u'^2(t) = \frac{1}{T} \int_0^T u_T(t)^2 dt \tag{41}$$

replacing the equation *40* in the equation 39 gives:

$$Ca = \frac{Pa - Pv}{\frac{1}{2}\rho(u_m^2(t) + 2 \cdot u_m(t) \cdot \delta u(t) + \delta u^2(t))}$$ (42)

If we assume that $\delta u(t)$ is proportional to the standard deviation of the measured values in the speed system, and that in turn, this standard deviation is a function of the average speed, (Gavilán, C.J. 2008) we find that:

- $\delta u(t)$ is zero for low speeds, therefore, the Y expression is accurate and can be applied to all fluid points. Moreover, the Bernoulli and Euler theorem is applicable, therefore, there will be no spontaneous cavitation, unless the average speed changes.
- For high speeds, $\delta u(t) >> 0$, there may be some speed values at which Ca is lower than the average value, and therefore, spontaneous cavitation may occur.

This effect will be called Fluid Induced Cavitation (FIC), given that, although cavitation is associated with turbulence, in turbo-machines or rotary pumps, little attention is paid to spontaneous cavitation due to the effect of turbulence on fluid systems. This effect is not widely known, though it is most definitely of great importance when dealing with fluids that are working very near the vaporization limit, or to put it more clearly, when the system pressure is very near the fluid vapour pressure at working temperature. This is particularly important for thermal power plants, or energy producing stations. In such facilities, the liquid is heated before entering the vaporization element; if there are elements that make the pressure fall, such as elbows, T's, filters, etc. in the conditions prior to vaporization, the numerator of equation 39 drops, reducing the Ca value, thus representing a high risk situation. In the same way, if we have elements in which the speed rises, such as jet pumps, venturi tubes, and other restrictions, the denominator increases, in such a way that the Ca value falls, thus increasing the risk of cavitation.
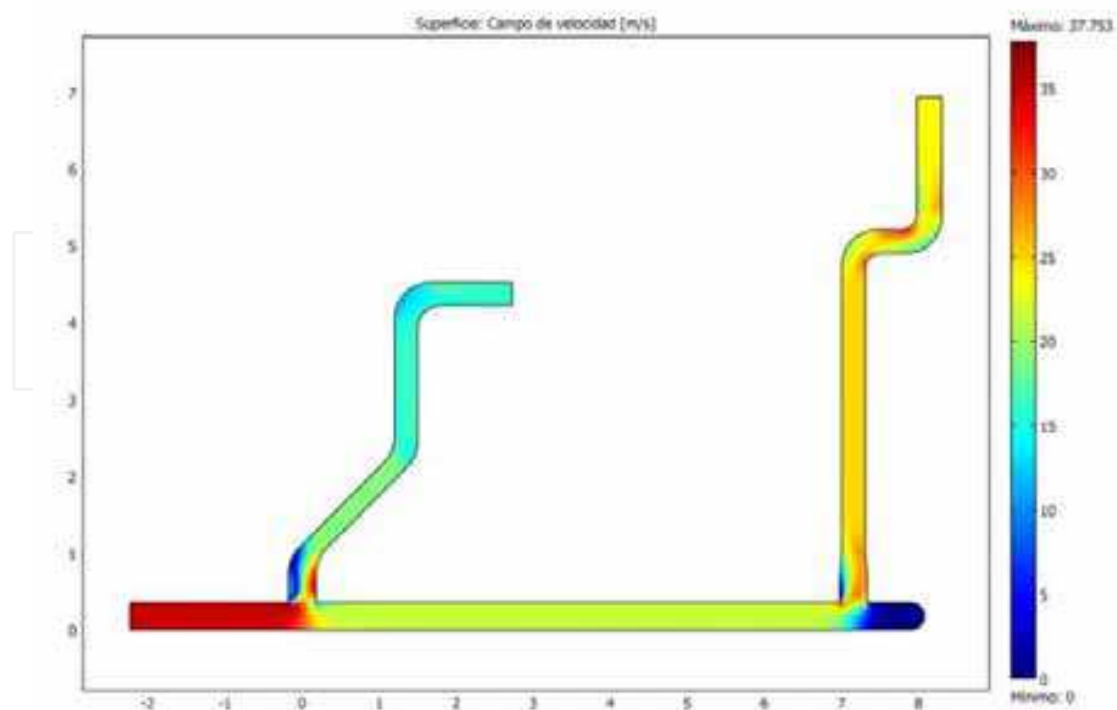

Fig. 4. Flow in pipe system.

Cavitation, which elsewhere and in other fora is referred to as *flashing*, is a vibration and noise - FIV and FIN - and may even manage to change the flow pattern, and therefore, cause FII flow instabilities. Other effects also need to be taken into account, such as the presence of erosion-corrosion, in what is, in principle, a single-phase fluid. Furthermore, if there are stable cavitation conditions, and a real and permanent void ratio is established, pump cavitation is ensured, even when this should not occur according to the calculations.

There are other reasons for possible cavitation, such as variations in the density and vapour pressure parameters on account of changes in the pressure and temperature conditions.

Let us have a look at a real example. Figure 4 shows the case of feed water speed in a pipe to an electricity-generating installation boiler. If we calculate the *Ca* parameter between two points, A and B, already having the average, or tendency, speed and the real one, we see that their *Ca* values are different. After the *Ca*, *v* and *p* values have been calculated in several situations, if we extrapolate them, there is such a turbulent speed value that it provokes spontaneous cavitation (Figure 5). Therefore, there is a speed limit for each flow at which spontaneous cavitation occurs, which coincides with the asymptotic value.
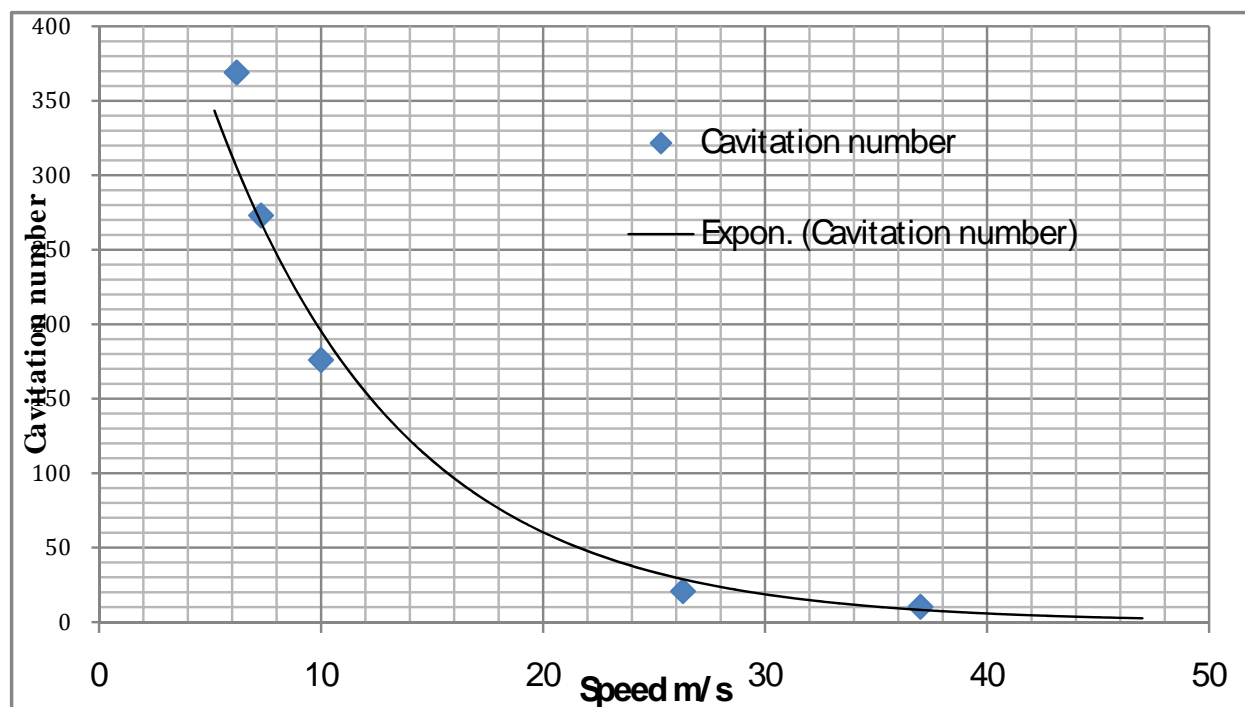

Fig. 5. Cavitation number versus flow speed.

The cavitation effect is not completely harmful, given that occasionally it is provoked by means of the speed of the fluid around a vehicle in such a way that movement resistance is very low and energy is saved in the movement, the fluid entry length is increased, or the energy is increased on knocking against another object in the fluid. This is the case of the supercavitating torpedoes used by the Russian navy.

4. Fluid Induced Vibration. (FIV)

There are lots of books and articles that have dealt with this subject. Strictly speaking, the term was only coined in the 1980's. In truth, this case study is a particular case of fluid-

structure interaction. Interest in this subject lies in the fact that the source of vibration is dissipated energy caused by turbulence, or in other cases, by eddies that produce oscillating lift forces that impregnate objects immersed in the fluid with a vibratory movement.

There are two basic FIV mechanisms:

- a self-induced vibrating mechanism
- a forced vibration mechanism.

Mathematically speaking, this is true. Nevertheless, the subject is somewhat wider than this might suggest, as can be seen from the following classification, which provides us with a more complete view. (Figure 6).

| Fluid and flow	Flow field	Vibration mechanism	Example
Single-phase flow	External flow	Vortex induced vibration (VIV)	• Resonant vibration • Forced vibration
		Acoustic resonance	• Acoustic resonance • Cavitation
		Fluidelastic vibration	• Wing flutter and galloping • Fluidelastic vibration of tube arrays
Steady flow	Internal flow	Surging	• Compressor surge • Pump surging
		Vibration of piping	• Piping, bellows, collapsible tubes
Unsteady flow	Pulsating flow	Forced vibration	• Vibration due to internal fluid oscillations
		Acoustically induced vibration	• Combustion-induced vibration
	Turbulent flow	Random vibration	• Buffeting • Vibration of reactor internals
	Sudden change in flow	Pressure pulsation	• Valve vibration • Water hammer
Two-phase flow	Bubble-induced vibration		• Sloshing
	Thermal-hydraulic vibration with phase change		• Vibration caused by condensation • Instability caused by boiling
	Vibration of piping by two-phase flow		

Fig. 6. Vibration mechanism.

As far as we are concerned, two of the most important effects, or examples, as regards nuclear plants of the Boiling Water Reactor (BWR) type, are those that reflect the influence of FIV on reactor internals. That is to say, on single-phase fluids in a non-stationary operating system with turbulent flow, and in the case of a bi-phase flow, those that are subject to FIV on account of the vibrations caused by the phase change, which may even go as far as to cause thermo-hydraulic instabilities.

Therefore, we will analyse two examples, fuel element vibrations in a flow with phase change and vibration induced by the leak flow in a BWR's jet pumps.

In the latter case, the jet pump FIV can be modelled as a vibration induced by the external axial flow. This is so because the leak flow through the Slip-Joint is deemed to be external to the mixer, as can be seen from Figure 7.
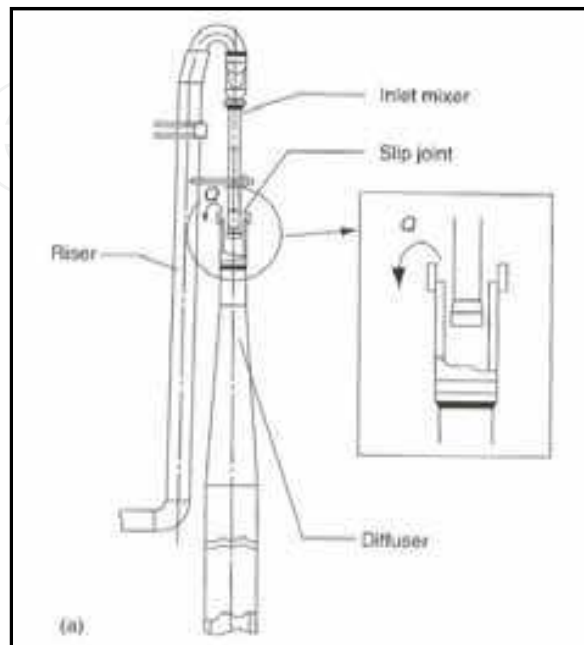

Fig. 7. JetPump and Slipjoint leak.

Thus, the model will be an axial flow cylinder, as described by Chen and Wambsganss (1970). The turbulent flow in the exterior, axial fluid gives rise to uneven pressure distribution on the outer wall of the pipe. Thus, on lacking balance it possesses resulting transverse forces. Moreover, as it is neither a permanent nor a stationary situation, the continuous change in pressure distribution over time, in space and in axial length, produces vibrations. The situation described is that which is shown in Figure 8.
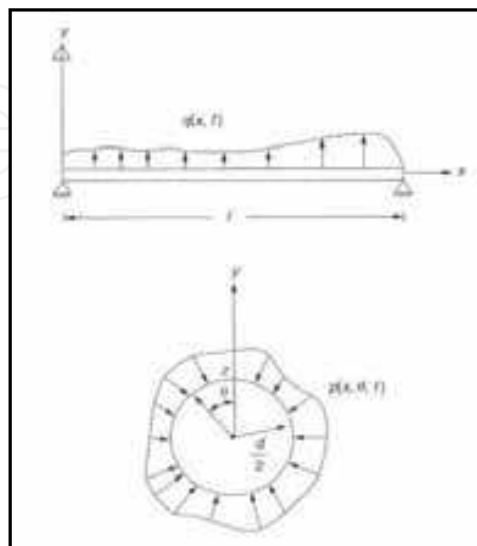
Fig. 8. Pressure distribution in an external flow pattern.

The Corcos (1963) model is used to analyse this type of situation. The model is expressed by:

$$\psi_{pp}(w, z_1, z_2, \theta_1, \theta_2) = \phi_{pp}(w) \cdot A\left(\frac{w|z_2 - z_1|}{V_c}\right) \cdot B\left(\frac{w \cdot D \cdot |\theta_2 - \theta_1|}{2 \cdot V_c}\right) \cdot e^{iw\frac{w|z_2 - z_1|}{V_c}} \quad (43)$$

where ψ_{pp} is the cross-spectral density of the pressure field, φ_{pp} is the pressure power spectrum at the point, A and B are spatial functions and V_c is the convection speed.
φ_{pp} value is given by:

$$\phi_{pp}(fr) = \begin{Bmatrix} 0.272 \cdot 10^{-5}/_{fr^{0.25}} \; si \; fr < 5 \\ 22.75 \cdot 10^{-5}/_{fr^3} \; si \; fr > 5 \end{Bmatrix} \quad (44)$$

where f_r is the reduced frequency, which is given by the following, where Dh is the hydraulic diameter:

$$fr = \frac{f \cdot Dh}{V} = \frac{w \cdot Dh}{2 \cdot \pi \cdot V} \quad (45)$$

The convection speed of the limit layer is given by:

$$\frac{V_c}{V} = 0.6 + 0.4e^{\left(-2.2 \cdot \frac{w \cdot \delta}{V}\right)} \quad (46)$$

where

$$\delta = \frac{Dh}{2(n+1)} \quad (47)$$

$$n = 0.125 \cdot m^3 - 0.181 \cdot m^2 + 0.625 \cdot m + 5.851 \quad (48)$$

$$m = \log(Re) - 3 \quad (49)$$

Lastly, the vibration amplitude is given by the approximations:

$$y_{rms} = \begin{Bmatrix} V^{1.5} \; si \; fr < 0.2 \\ V^2 \; si \; 0.2 < fr < 3.5 \\ V^3 si \; 3.5 < fr \end{Bmatrix} \quad (50)$$

These equations result in the generation of transversal forces, which move the mixer parts, the elbows and the riser. Moreover, as a result of its geometrical configuration, mode 3 vibration causes damage as a result of the stress at the first fixed point of the system, which is the joint between the riser and its support. Indeed, it is this stress that provokes breakages. A detail of the turbulence associated with the simulation of slipjoint leak can be seen in Figure 9.
In general, the Païdousis (1973) model is the equation used for industrial settings.
As far as FIV caused by external flow with phase change is concerned, its study and development can basically be put down to the nuclear industry, after the development of boiling water reactors. At such plants, boiling occurs on the external part of fuel rods in the upflow. This study was later extended to the steam generator pipes of pressurised water reactors. Figure 10.
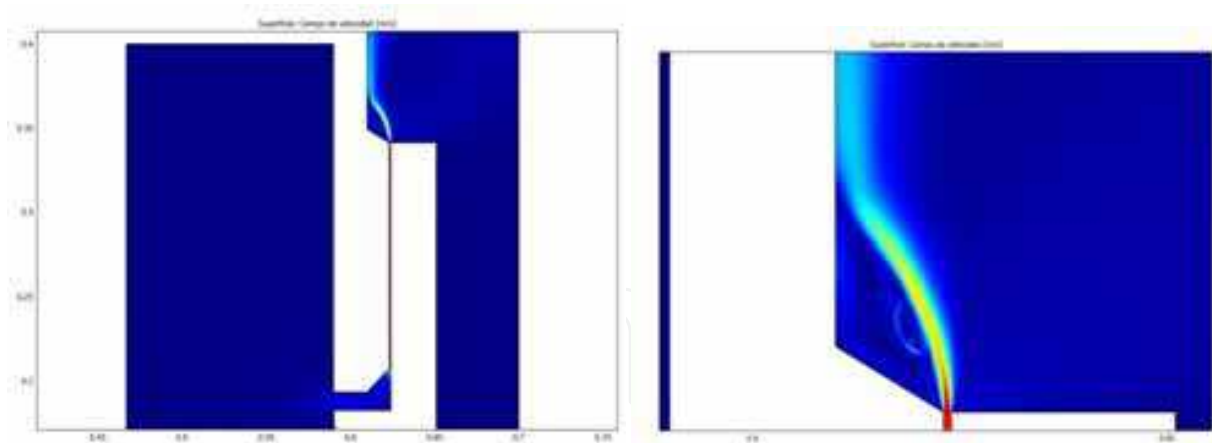
Fig. 9. Simulated Slipjoint leak and vortex induced.
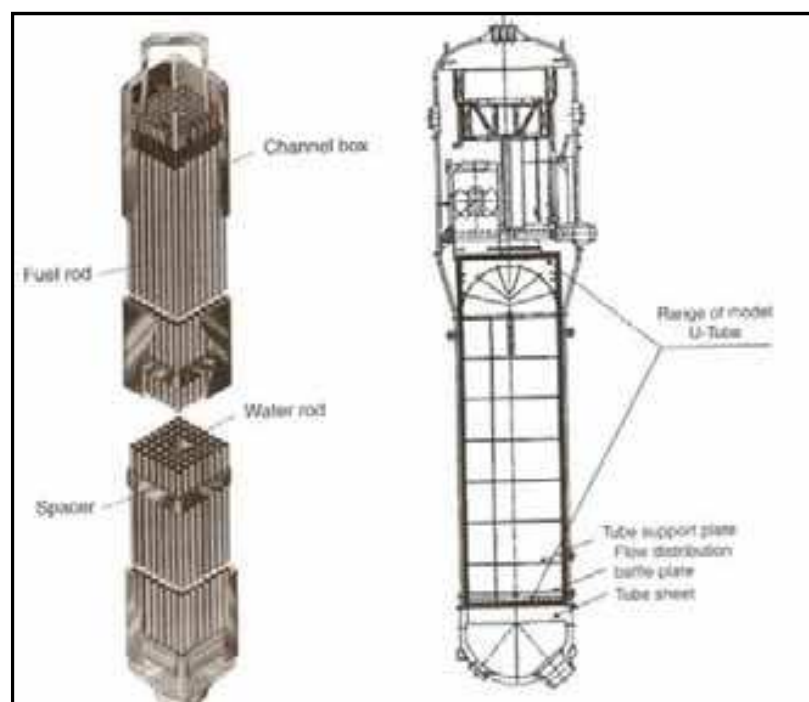

Fig. 10. Fuel Bundle and Steam Generator.

Both studies reached the same conclusion, namely that the vibration amplitude is proportional to the mass upflow, but decreases with pressure. As far as fluid quality, or the void ratio, is concerned, two peaks can be seen, 0.1-0.25 and 0.4-0.5, which suggests that there is great dependence between vibration amplitude and the void ratio, or fluid quality.

On a BWR (Figure x) type fuel bar, it was established that the pressure power spectrum of the excitation force is proportional to $V^{1.56-2.7}$, while the amplitude is proportional to $V^{0.78-1.35}$. These values were determined in a rod test carried out by Pettigrew and Taylor [13] under the following conditions:

Pressure: 2.8-9 MPa

Mass flow: 0-4600 Kg/m²s

Power: 1-1000 Kw

Quality: 0-0.25.

Saito (2002) came to the same conclusions in another test under different conditions.

5. Fluid Induced Noise (FIN)

In this section, we will take a look at the noise generated by a turbulent flow. Throughout this chapter and the following sections, fluid dynamics is based on movement equations, with speed as the unknown, essential analysis value.

For this particular case of noise induced by turbulence, a change of mindframe is called for in the sense of assessing the fluid in terms of pressure, and even density. Original FIN theory and expressions are given by the Ligthhill aeroacoustic model (1952/1954), as indicated below:

$$\nabla p^2 - \frac{1}{c_0^2} \frac{\partial^2 p}{\partial t^2} = -\frac{\partial^2 T_{ij}}{\partial x_i \partial x_j} \tag{51}$$

$$T_{ij} = \rho v_i v_j \tag{52}$$

where T_{ij} is the turbulent stress tensor. Whenever the fluid can be compressed, pressure variation is accompanied by density variation, the expression of which is:

$$\frac{\partial^2 \rho}{\partial^2 t} - c_0 \frac{\partial^2 \rho}{\partial x_i \partial x_j} = \rho_0 \frac{\partial^2 v_i v_j}{\partial x_i \partial x_j} \tag{53}$$

Thus, turbulence collaterally generates pressure and density variation in the fluid. By means of the turbulent stress tensor the turbulence produces variations in pressure and density. The former cause the noise, and as such, are deemed to be sound sources.

There are many practical applications of the analysis of turbulence generated noise. Two particularly curious, albeit useful ones, have solved some serious problems. The two situations in question are:

- Determination of leaks through the seat of safety relief valves from the outside by means of non-intrusive techniques.
- Element breakage due to resonance frequencies.

The first of the above situations has been used to detect safety relief valve leaks in BWR nuclear plants. The theoretical principle employed is that the seat leak flow produces turbulence which in turn generates a characteristic sound. The conceptual model is similar to the one used by Van Herpe and Creghton (1994), in which they model the fluid flow through a conduit with a restriction inside. These researchers came to the conclusion that the acoustic power, dB, is proportional to the speed in the conduit and to the passage diameter determined by the restricting element. Consequently, an SRV leak can be detected by means of sound and its register, but also by its evolution. The latter claim is based on the tests done by EPRI on this particular study NP-2444-SY. In this study, the frequency band is established at which the leak is best detected, 40-55 KHz, as well as the complete detection interval, 30-60KHz. Likewise, the author holds that regular monitoring can establish drift and trend patterns, the development mathematical law of which is that determined by Van Herpe y Creghton (1994).

The other case refers to the catastrophic breakages of steam dryers at BWR plants due to an acoustically sourced resonance. (Figure 11).

After the failure of the Quad cities dryer, a study was carried out on the loads to which it was subject. In none of the cases did the operating loads justify the breakage, or degradation, of the component. Consequently, a study was made of the vibratory or pulsatory phenomena, by measuring the vibrations at the component and the passage of

pressure along the main steam lines. Acoustic excitation coming from the main steam lines is the current model. (Figure 12).
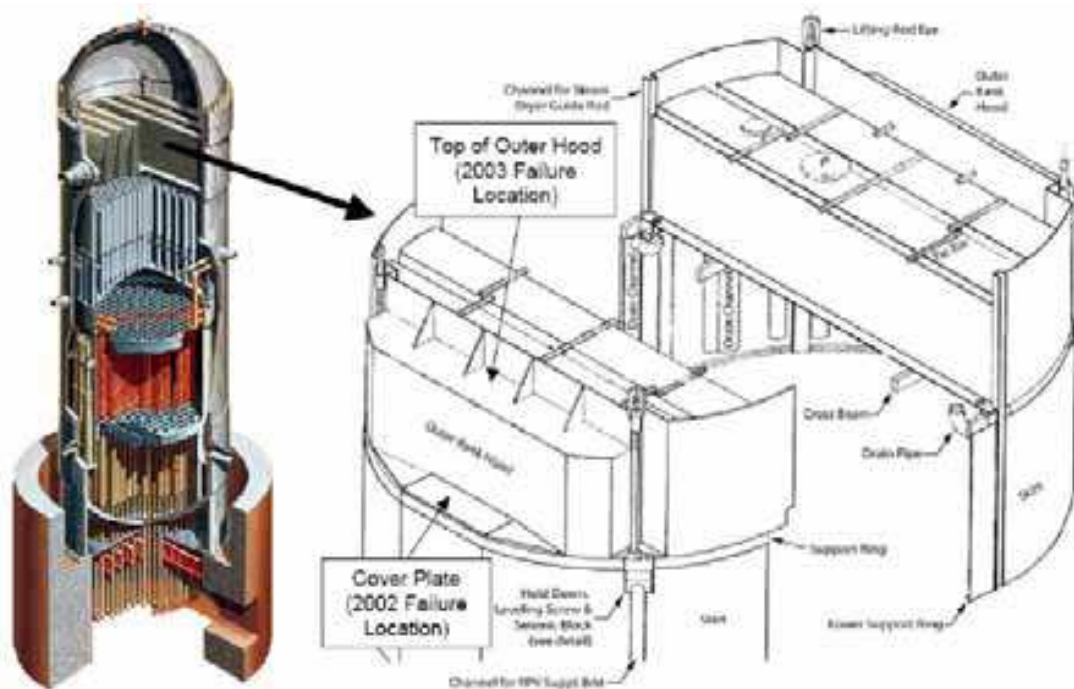
Fig. 11. BWR vessel and Steam dryer detail. (Cracked areas)
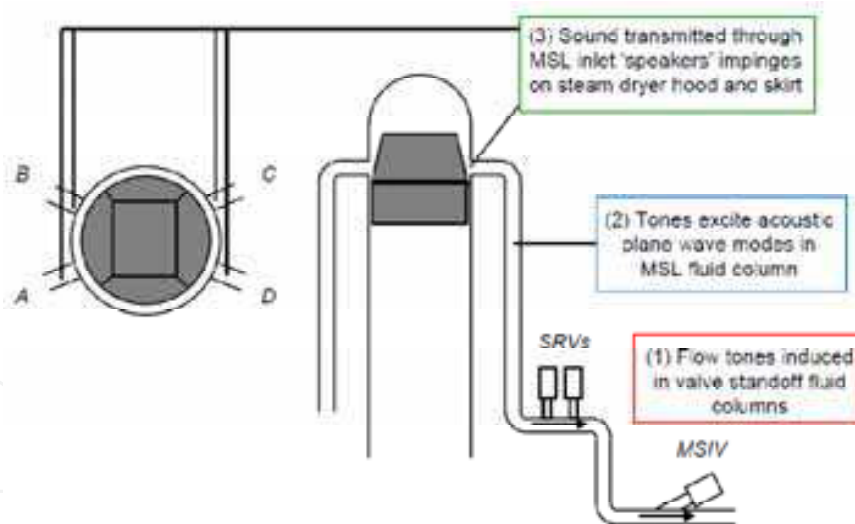
Fig. 12. MSL, SRV's and the main characteristic of the sound transmission.

Acoustic excitation is produced in the main steam lines as a result of the turbulence generated at the SRV connections, instrumentation connections, equalising header, etc… (Figure 13)

This turbulence, which in general, manifests itself as vortices or eddies will, in the Von Karman sense, give off a determined frequency. Moreover, the lower scale turbulence will have its own frequency in accordance with the Lighthill model. Thus, the pressure waves that are generated with a defined frequency will constitute an external dryer load that increase its total dynamic load. (Figure 14).
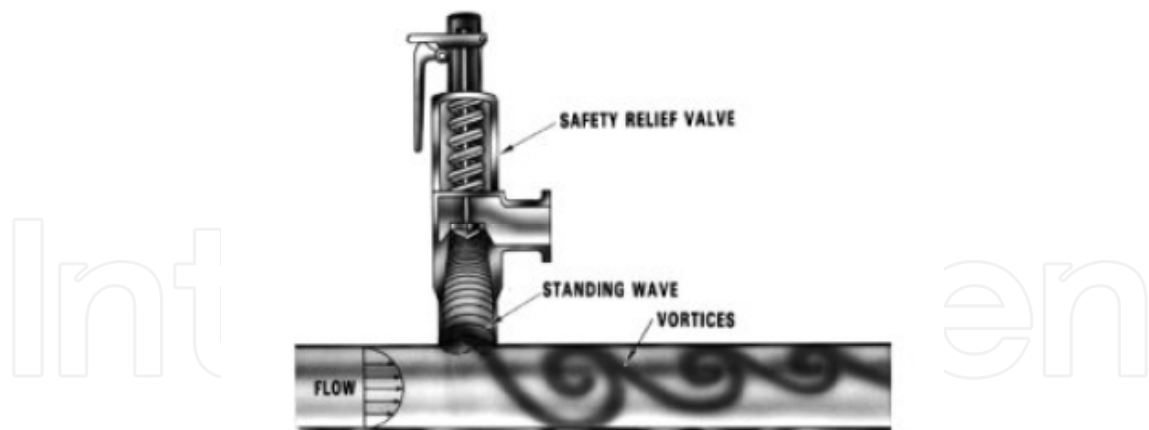
Fig. 13. Singing branch. Vortex Sheeding.
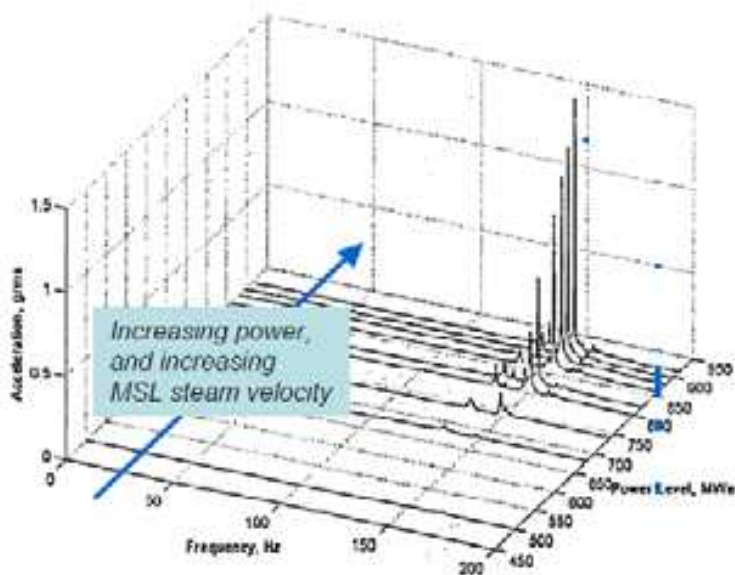
Fig. 14. Frequency dependency of the power and acceleration of the induced load.

Moreover, this load with be pulsatory in nature and will have a determined frequency, thus, if it coincides with a natural dryer frequency, the pressure effects are amplified, exceeding the resistance of the material, in some cases breaking, in others causing cracks.

As can be seen, there are frequencies in Figure 14 that coincide with certain natural ones of parts of the dryer (Figure 15). Consequently, there will certainly be damage. The only variable will be time and the power of the vibration due to the reactor power. Notwithstanding, the solution to the problem is to be found at the same source as the excitation, namely, by studying the turbulence. It has been proven that by changing the geometry of the SRV connection, this changes the spectrum frequency, and consequently, the effect on the dryer. (Figure 16).

In line with the practical focus followed in this chapter, there are reduced analytical studies that make it possible, in a T-type geometry, to predict and check the existence of acoustic excitation applied to steam pipes.
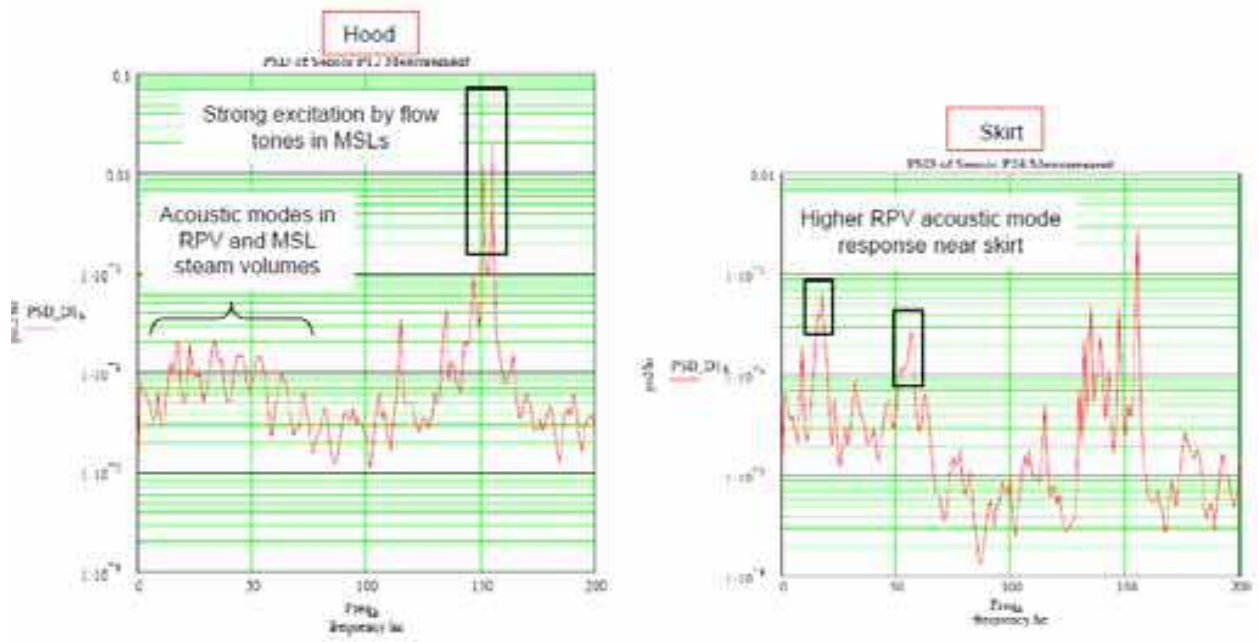
Fig. 15. Natural frequencies of the steam dryer Hood and skirt.

Fig. 16. Acoustic side branch, and the effect on the pressure, or load.

The mathematical expression is:

$$S_0 = \frac{a \cdot N \cdot (d+r)}{4 \cdot L \cdot V_0}$$ (54)

where:
S_0 is the Stroudhal number;
a is the speed of sound in a fluid medium;
N takes on value of 1 and 3;
d is the branch diameter;
r is the branch curve radius at its connection to the main line;
L is the branch length;
V_0 is the main line speed.
The assessment is carried out in accordance with the Strouhal number, defined by the equation x, if the value lies within the 0.25-0.60 interval, for which it can be said that there is a big likelihood of acoustic excitation appearing. The frequency estimate can be approximated by the following function:

$$S_0 = \frac{f_s \cdot d}{V_0}$$ (55)

6. Fluid induced instabilities.

In this section, we are going to deal with fluid instabilities, though more specifically with that which makes the flow bistable, given that this represents a transition within the turbulent system. Notwithstanding, what follows is a brief description of other instabilities about which references and studies abound. Turbulent flow, as has been above, is a generalised process, whereas instability is different. This is an unexpected situation, and one which, in principle, should not be happening. Quite often it is associated with the local formation of turbulence in a laminar, ordered flow. The most widely known instabilities model and study turbulence of this type of situation, but there are other instabilities in a turbulent flow that cause changes to the flow pattern. As with turbulent flow and its transition, instabilities possess factors that give rise to same, which are:

- Fluid-structure interaction: Remodels the flow
  - Von Karman
  - Stroudhal
- Density or viscosity variations
  - Raleigh-Taylor
  - Plateau-Railegh
  - Ritchmyer-Meshkov
- Speed difference
  - Kevin-Heltmotz.
- Increase in turbulence intensity
  - Bistable flow.

All of these instabilities exert different effects on the structure that is either immersed in them, or that contains the flow, such as vibrations, noise or change in process flow values. The latter, is of itself only an instability, albeit a very perculiar one, thus it will be dealt with separately. The others, given their spatial characteristics, have been dealt with separately in Sections 4 and 5.

Presented here is an important advance on the investigation of the bistable flow phenomenon inside a boiling water reactor (BWR) vessel. The study of the flow time series concludes that the phenomenon of the bistable flow is a particular case of transitions induced by turbulence. Afterwards the phenomenon is identified, simulated and the model is validated. The real behaviour is reproduced using the mathematical model, which has given excellent results. Therefore the bistable flow is an instability that comes by transitions induced by turbulent flows and vortex.

During this analysis a new technique was used to characterize the phenomenon. The new technique was the Hilbert´s transform. The conclusion that came from this last study is that:

- The bistable flow is non linear and non stationary
- The bistable flow is produced when the plant is near the coast down and the flow is the maximum
- There is a relationship between the average value of the flow and the bistability.
- The bistable flow has two attractors structure.
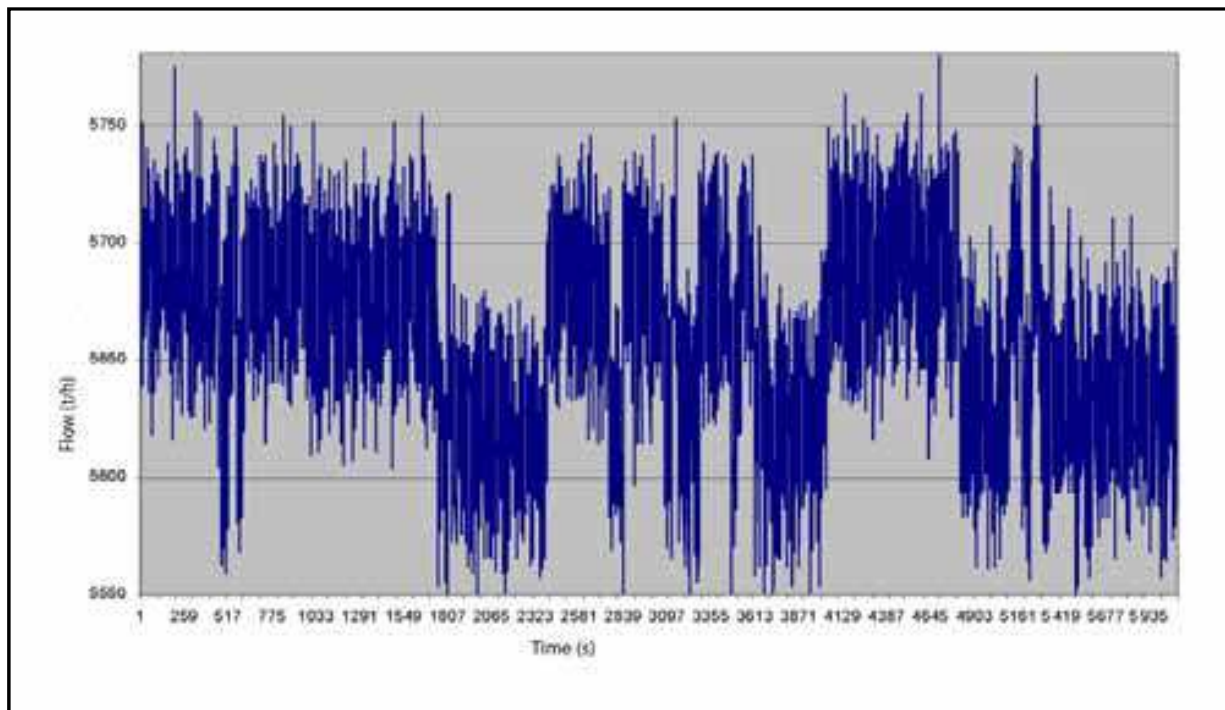
Fig. 17. Flow rate time series of in the recirculation loop. Bistable event.

One of the most absurd process features is that the white noise can induce order in a system that is non linear and non stationary, is not in equilibrium. That is, a chaotic system can be ordered by itself. This is called vibration resonance (Horsthemke, 2005), with transitions induced by noise. In this case the word noise and turbulence will be similar. So this phenomenon is modeled by the Laugevin´s equation (56).

$$\dot{x}_i = f(x_i) + g(x_i) \cdot \varepsilon(t) + \frac{D}{2 \cdot d} \Sigma\left(x_j - x_i\right) + A\cos(w \cdot t) + B\cos(\Omega \cdot t) \qquad (56)$$

Where:
x(t)i is the state of the i-esim oscillation.
ε(t) it is a gaussian noise zero-averaged an non correlated.

Fig. 18. Results of the Hilbert´s Transform. Real Time series (central), Phase (bottom), Inst. Frequency (upper)

The last terms in the equation, represent the external and periodic forces represented as low frequency and amplitude A, and another of high frequency with amplitude B.
For the case under study the expressions of the functions g(x) and f(x) are:

$$g\,(x) = K1x \tag{57}$$

$$f\,(x) = -\,K2x\text{-}K3x3(7) \tag{58}$$

For the above-mentioned the equation of the flow would be in the way:

$$\dot{x}_i = \varepsilon \cdot K_1 \cdot x - K_2 \cdot x - K_3 x^3 + \sqrt{\eta} \cdot \zeta \tag{59}$$

Resuming:

$$\dot{x}_i = x(\varepsilon \cdot K_1 - K_2) - K_3 x^3 + \sqrt{\eta} \cdot \zeta \tag{60}$$

Simplifying:

$$\dot{x}_i = x \cdot K_1' - K_3 x^3 + \sqrt{\eta} \cdot \zeta \tag{61}$$

Where:

x(t) is the flow and ζ is the zero averaged and non-correlated noise white. The parameters K1' and. K3 will be calculated to determine the times in those that, statistically, the system is in each value, or also called escape times.

To determine the values of the K´s factors it must be consider that:

- The averaged value of the flow is 5650 t/h and if there´s no noise or turbulence the results of the equation (61) are zero.
- The averages deviations of the average value must be +50 and -50 t/h.

The values of the parameters expressed in the equation (61) and that are coherent with the previous premises are given by the table 2.

Parameter	Value
K1`	0.0052
K2	8e-11
η	0.1797
Desv. Typical Noise	40

Table 2. Values of parameter to equation (58).

The realization of the equation (61), gives results such the follows, showed in figure 19 and 20.
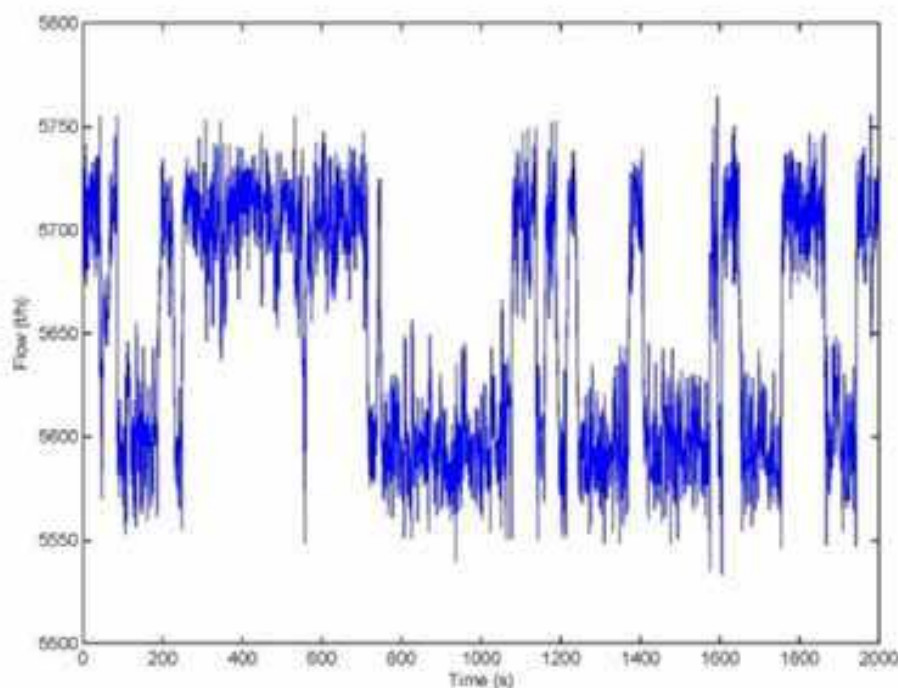
Fig. 19. Realization of the equation (61) with the parameters of the table 2.
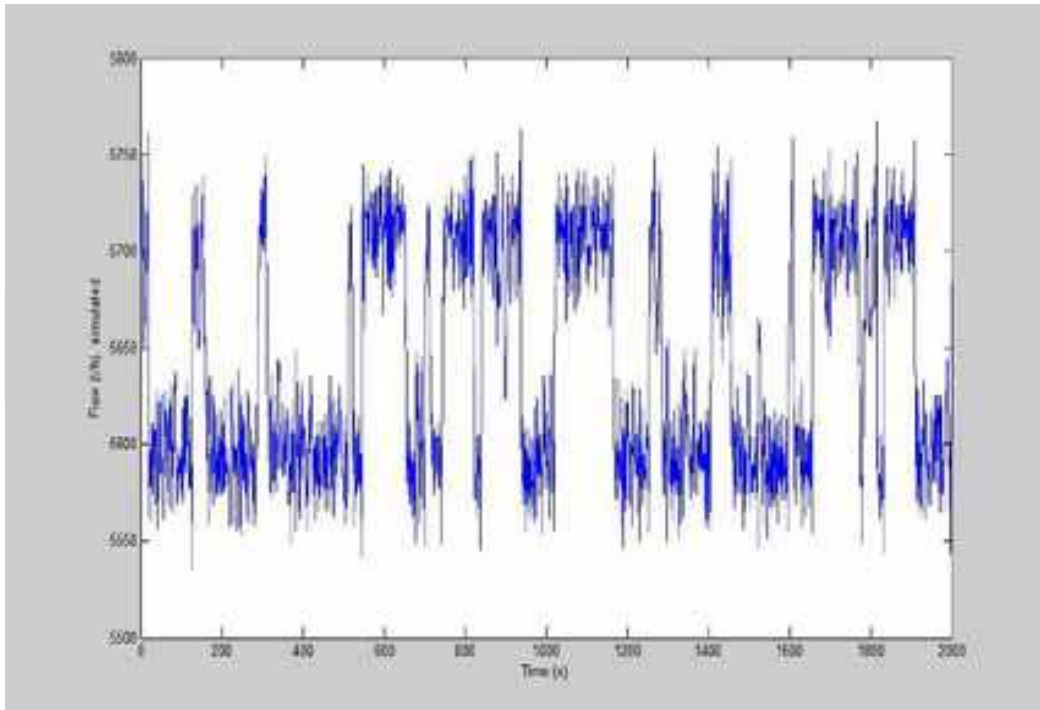
Fig. 20. Realization (2nd) of the equation (61) with the parameters of the table 2.

The previous graphics are two drawings of the flow value in sets of 2000 samples, in order to have a more representative graphic.

The difference between the simulation and the real time series is due to the measurement method that adds a new noise to the signal, but that noise is not important to the phenomenon. The flow is measured by the difference of pressure in an elbow, so in this method the centrifugal force has to be measured and then the mass flow.

The validation is based in two steps. The first step is the generation of the histogram, autocorrelation graphic and the spectral density graphic (figures 21, 22 and 23) to compare with the results showed in the characterization previous work done by Gavilán (2007). And the second is the evaluation of the phase diagram given by the Hilbert´s transform over the simulated data and the comparison with the real data phase
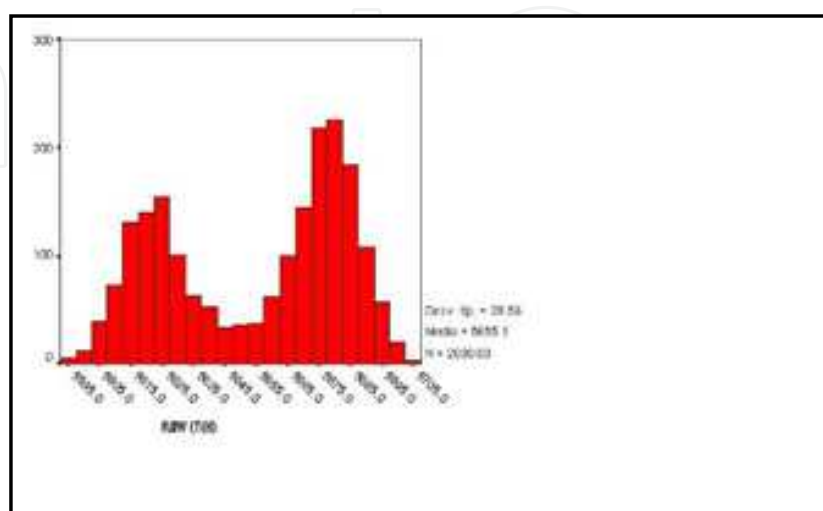
Fig. 21. Simulated time serie Histogram. (2000 seconds)
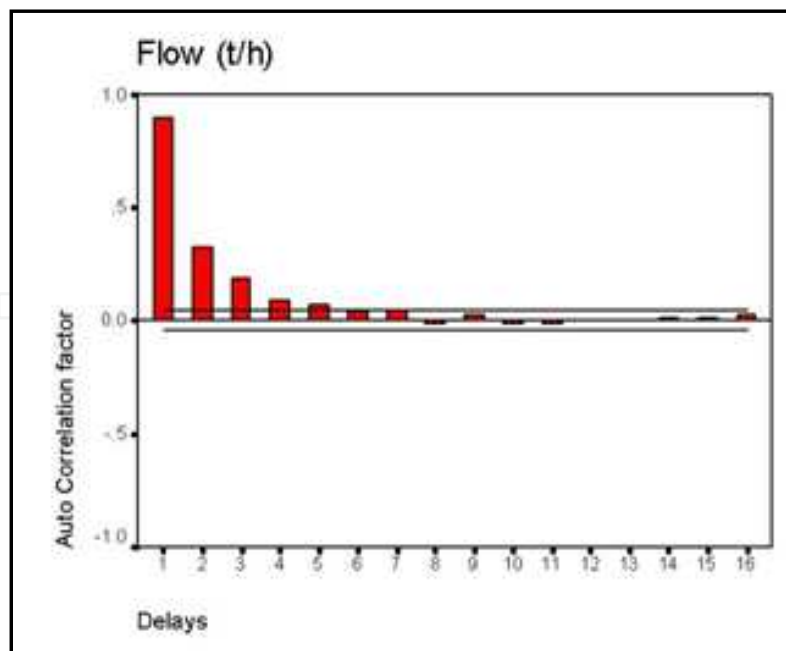
Fig. 22. Simulated time serie Autocorrelation factor
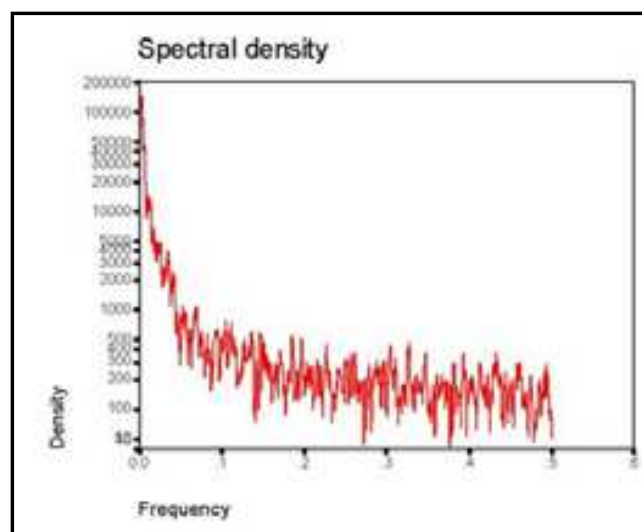
Fig. 23. Simulated time serie Spectrogram.

The statistic parameters of the simulated series, (from figures 21, 22 and 23) are coherent with the results found by Gavilán (2007) in the characterization of the bistable flow signal.

To conclude the validation method, is necessary to check if the simulated time series have the same characteristics as the real one in the Hilbert´s sense. So to compare is necessary to repeat the Hilbert´s transform but now to the simulated time series. The results are showed in the figure 24.

In the figure 124, y can be observed the structure of two attractors in the phase, and in the instantaneous frequency. The law for the transitions between one and the other attractor, in the phase space, is an arcos(K(t)) and the instantaneous frequency is the derivate of it. If we compare the figures17, 18, 19, 20 and 24 can be concluded that the simulated series adjust fairly to the real one. The adjustment appears very qualitative but must remember that the relationship in statistical.
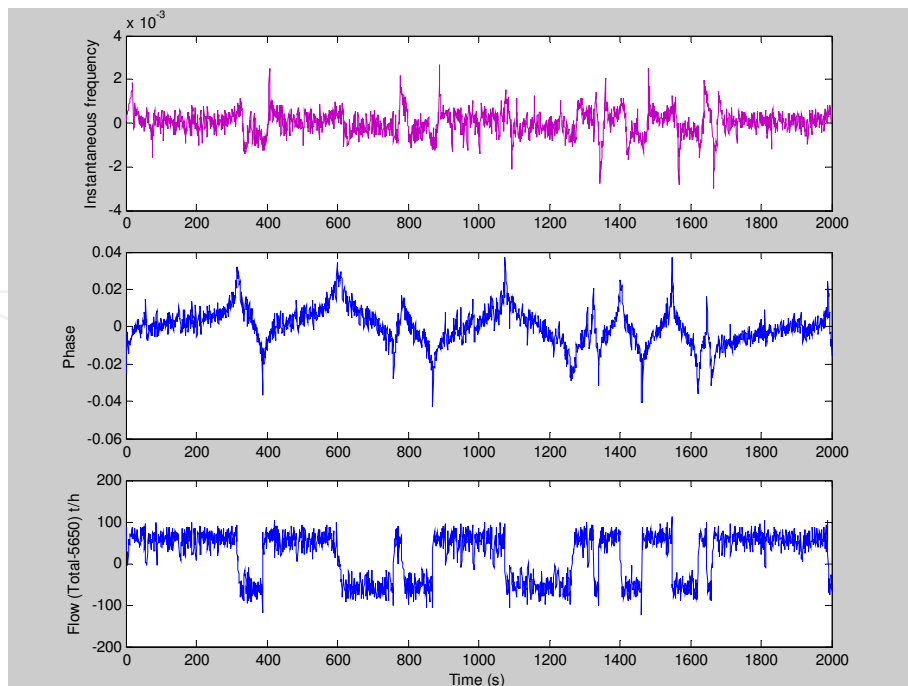
Fig. 24. Results of Hilbert´s transform to simulated data.

The characterization of the bistable flow results in, that is non linear and non stationary process. The bistable flow can be evaluated and characterized, properly using the Hilbert´s Transform.

The bistable flow appears under some operative conditions without change in the values of control variables, so is associated to an internal variation. The variation is due to the turbulence that is a self oscillatory process in a continuous medium. The development of a turbulence event is the birth of an attractor in the space of the phase. The turbulence is a convective process because it doesn´t increase indefinitely but rather it evolve to water bellow. All those conclusions about the turbulence justify that the flow change the average value of the speed and then the value of the flow taking one of the two values of the attractor.

The turbulence is an unstructured process, because there´s no pattern in it. The Fourier transform gives poor results when is used so that´s the reason why the turbulence is associated to a noise, and sometimes to a white noise. The phenomenon of bistable flow is a turbulence induced transition process, because the reason of the jumping between two flow values is the turbulence. Because turbulence and noise are physically the same, mathematically the phenomenon can be simulated with a noise-induced transition model.

The simulation gives us, a low error simulated time series that had the same statistical parameters than the original. And the other idea is that the bistable flow only appears in a finite region of the flow space, because there´s only a set of values of the turbulence and flow that induce the bistable behavior. In the same idea, the noise (turbulence) has only one value to induce the bistable flow. The characteristics parameter of the noise is the average that must be zero, and the standard deviation that has a relationship with the value of flow, and only in a small interval of values produce the bistable flow (table 3, figure 25). The relationship between the noise standard deviation and the flow depends in every installation because depends on the hardware but in this case can be modeled by the equation (62).

$$StdDev(F) = 30.02 + \frac{A}{\dfrac{B^2}{Flow(t/h)^2} - 1} \qquad (62)$$
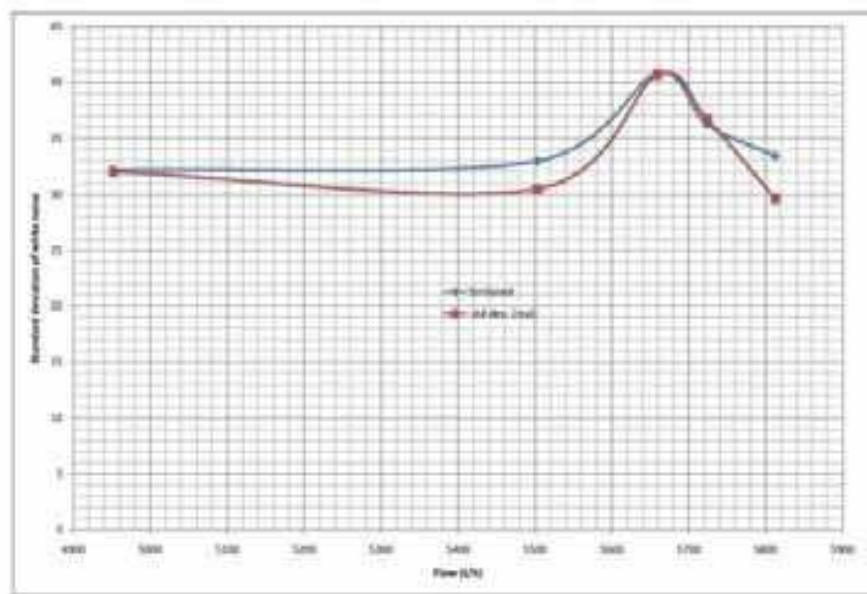
Fig. 25. Relationship between average flow and noise typical deviation.

Interval Time	Min. Flow (t/h)	Max. Flow(t/h)	Average Error	Typical Deviation	R2 adjusts lineal	Bistability
300-1200	4423.9	5479.2	4.17	32.01	0.9844	No
1500-3000	5323.3	5682.9	-41.01	30.47	0.7952	No
3001-10000	5492.7	5825.7	0.091	40.71	0.5011	Yes
10001-13000	5579.9	5867.7	0.055	36.72	0.2972	Yes, smaller
13001-15000	5695.3	5929.5	0.0455	29.63	0.1482	Residual

Table 3. Parameters of several intervals of flow and conditions.

7. Conclusion

This chapter has shown that turbulence exercises several effects in the industrial setting, and except for those of diffusion, or mixture, all the others are both harmful and give rise to problems. Given its variety and applicability, it is not easy to discover the reason for a component failure. Sometimes, only an in-depth analysis of the problem from the perspective of turbulence can serve to clarify a case that defies normal analyses.

Therefore, a thorough grounding in fluid mechanics is needed to solve the problems related to turbulence. Furthermore, a knowledge of computer fluid flow modelling tools, which

involves so-called Computational Fluid Dynamics (CFD), represents a great advance in the knowledge of the turbulent behaviour of fluids in movement. Notwithstanding, all is not science and mathematics, given that turbulence is chaos, and therefore, there will always be a certain druidic facet in those professionals given to working in this field.

As an end to this chapter, we provide a summary table (Table 4) that can serve as a guide to locating what effect may be producing the turbulence, with the aim in mind of better focusing the subsequent analyses.

Fluid type // condition	Turbulence effect	Affected area
Single-phase // Saturated fluid	Cavitation	Venturi tubes and geometry changes
Single-phase fluid	Instability	Connection geometry
	Noise // Acoustic Excitation	Connection geometry
Fluid structure	Vibration	Elements submerged in the current
	Noise // Acoustic Excitation	Elements submerged in the current

Table 4. Summary of fluid type and effects.

Lastly, a look at the use of CFD´s. The use of this type of tool does not ensure the success of the study, given that employing it a preliminary analysis needs to be done and the following defined:

- Model type (LES, RANS, DNS…)
- Minimum modelling scale (Kolmogorov)
- Analysis type (permanent or provisional system)
- Variable to be simulated (density, pressure or speed)

Otherwise, the results from the computer will be nothing more that a nicely coloured drawing, without any coherent information.

"Linearity is an idea sought after, yearned for and forced by the human mind. It is a reflection of our condition as animal. Only by accepting, assimilating and understanding the chaos of the world that surrounds us, will we truly ascend to the rational condition."

8. References

United Stated Nuclear Regulatory Commision. (1986). Anomaluos behavior of recirculation loop flow in jet pump BWR plants, Information. *notice No. 86-110*. Washington.

A. Nuñez Carrera, E. Martinez-Mendez, G. Espinosa Paredes (2006), Análisis del fenómeno de flujo biestable de la central Nucleoeléctrica de Laguna Verde. *Proceedings of the 2006 Congreso Internacional Buenos Aires. LAS/ANS.*

C.J Gavilán Moreno (2007). El flujo biestable en lazos de recirculación de una central BWR. Analisis y caracterización. *Proceeding of the XXXIII Reunión anual de la Sociedad Nuclear Española.*

C.J. Gavilan Moreno, (2008) Analysis and simulation of the flow signal in the recirculation loop of a nuclear power station during a bistable flow event. *Nuclear engineering and Design*. Vol 238, Issue 10, pp-2754-2760.

C.J, Gavilán Moreno (2009) Hydraulic study on recirculation loops using computational fluid dynamics (CFD). Design optimization and turbulence reduction. *Nuclear Engineering and Design,* Volume 239, Issue 3, pp 434-441

N.E Huang, Introduction to the Hilbert-Huang transform and its related mathematical problems. *Goodard Institute for Analysis dates*. NASA.

S. Ziada, S. Shine. (1999). Strouhal numbers of flow excited acoustic resonance of closed side brances. *Journal of fluids and structures*. Vol 13. 127-142.

R.M. Baldwin H.R. Simmons.(1986). Flow induced vibration in safety relief valves. *Journal of pressure vessel technology*. Vol.108. Pp. 267-272.

O.C. Zienkiewicz; R.L. Taylor   (2004) *El método de los elementos finitos. Vol. 3, dinámica de fluidos*. Ed. CIMNE.

K. Morgan, E. Oñate, J. Periaux, J. Peraire and O (1993) *Finite element in fluids. New trends and applications.* Ed. CIMNE.

Lesieur. M (2008) *Turbulence in fluids* Ed. Springer.

Horsthemke & Lefever (2005). *Noise Induced Transitions.* Ed. Springer series in Sinergetics.

White, Frank M. (2008) *Mecánica de fluidos*. Ed. McGraw-Hill.

D'Agostino-Salvatore Eds (2007) *Fluid Dynamics of Cavitation and Cavitating Turbopumps*. Ed. SpringerWien NewYork.

Persson, Per-Olof. (2002) *Implementation of finite element based Navier Stokes Solver.* 2094 Project.

Bigersson, F.; Finnveden, S. ; Robert, G. (2004) Modelling turbulence induced vibration in pipes with a spectral finite element method. *Journal of sound and vibration*. Vol 278. Pp 749-772.

Kolmogorov, A.N. (1941) The local structure of turbulence in incompressible viscous fluid for very larger Reynolds numbers. *Proc. R. Soc Lond. A.* Vol 434, pp 9-13.

Roshko, A. (2000) On the problem of turbulence. *Current Science*, Vol 76, No 6, pp 834-839.

Dassé, J.; Mendez, S.; Nicoud, F () Large-Eddy Simulation of Acoustic Response of a perforated plate. *American Institute of Aeroanutics.*

Van Herpe,F.; Crighton, D.G. (1994) Noise generation by turbulent flow in ducts. *Journal de Physique III,* Vol 4. Pp 947-950.

Davies, P.; Holland, K.R.; (2004) Flow Noise generation in expansion chambers. *Procc of the Institute of Acoustic.* Vol. 26. Pt. 2, pp 206-213.

Hamakawa, H. et all (2006) Effects of flow induced Acoustic resonance on vortex shedding form Staggered tube banks. *JSME International Journal*. Series B, Vol. 49, No. 1, pp 142-151.

Chen, S.S.; Wambsganss, Jr. M.W. (1970) Response of a flexible rod to near field flow noise. *Proceedings of the conference on flow induced vibrations in reactor system components.* ANL-7685 Argonne National Laboratory.

Corcos, G.M. (1963) Resolution of pressure in turbulence. *J. Acoustic Soc. Am.* Vol 35, No 2 pp 192-199.

Païdoussis, M.P. (1973) Dynamics of cylindrical structures subjected to axial flow. *Journal of Sound and vibration. Vol.* 29, No 3, pp 365-385.

Saito, N. et all. (2002) BWR 9x9 Type Rod Assembly Thermal Hydraulic Test (2) – Hydraulic Vibration Test. *10th International Conf. on Nuclear Engineering*. ICONE10-22557.

Lighthill M. J., (1952) On Sound Generated Aerodynamically. I. General Theory, *Proc. R. Soc. Lond*. A 211 pp. 564-587.

Lighthill M. J., (1954) On Sound Generated Aerodynamically. II. Turbulence as a Source of Sound, *Proc. R. Soc. Lond*. A 222 pp. 1-32.
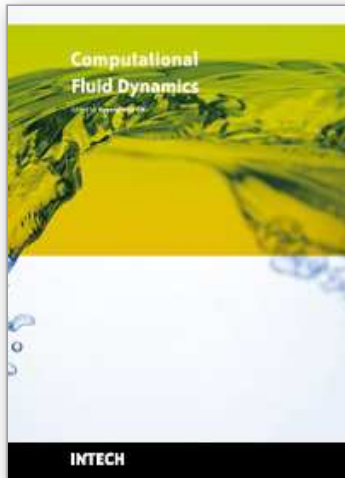
Computational Fluid Dynamics

Edited by Hyoung Woo Oh

This book is intended to serve as a reference text for advanced scientists and research engineers to solve a variety of fluid flow problems using computational fluid dynamics (CFD). Each chapter arises from a collection of research papers and discussions contributed by the practiced experts in the field of fluid mechanics. This material has encompassed a wide range of CFD applications concerning computational scheme, turbulence modeling and its simulation, multiphase flow modeling, unsteady-flow computation, and industrial applications of CFD.

How to reference

In order to correctly reference this scholarly work, feel free to copy and paste the following:

Carlos Gavilán Moreno (2010). Turbulence, Vibrations, Noise and Fluid Instabilities. Practical Approach., Computational Fluid Dynamics, Hyoung Woo Oh (Ed.), ISBN: 978-953-7619-59-6, InTech, Available from: http://www.intechopen.com/books/computational-fluid-dynamics/turbulence-vibrations-noise-and-fluid-instabilities-practical-approach-

INTECH
open science | open minds